Cerebral Cortex, April 2018;28: 1516–1531

doi: 10.1093/cercor/bhy018
Advance Access Publication Date: 6 February 2018
Original Article

ORIGINAL ARTICLE

Rab23 Regulates Radial Migration of Projection Neurons via N-cadherin

Catherine H.H. Hor[1,2] and Eyleen L.K. Goh[1,2,3,4]

[1]Neuroscience Academic Clinical Programme, Duke-NUS Medical School, Singapore 169857, Singapore, [2]Department of Research, National Neuroscience Institute, Singapore 308433, Singapore, [3]Department of Physiology, Yong Loo Lin School of Medicine, National University of Singapore, 8 Medical Drive, Singapore 117597, Singapore, and [4]KK Research Center, KK Women's and Children's Hospital, Singapore 229899, Singapore

Address correspondence to Eyleen Goh, Neuroscience Academic Clinical Programme, Duke-NUS Medical School, 8 College Road, Singapore 169857, Singapore. Email: Eyleen_Goh@nni.com.sg

Abstract

Radial migration of cortical projection neurons is a prerequisite for shaping a distinct multilayered cerebral cortex during mammalian corticogenesis. Members of Rab GTPases family were reported to regulate radial migration. Here, in vivo conditional knockout or in utero knockdown (KD) of Rab23 in mice neocortex causes aberrant polarity and halted migration of cortical projection neurons. Further investigation of the underlying mechanism reveals down-regulation of N-cadherin in the Rab23-deficient neurons, which is a cell adhesion protein previously known to modulate radial migration. (Shikanai M, Nakajima K, Kawauchi T. 2011. N-cadherin regulates radial glial fiber-dependent migration of cortical locomoting neurons. Commun Integr Biol. 4:326–330.) Interestingly, pharmacological inhibition of extracellular signal-regulated kinases (ERK1/2) also decreases the expression of N-cadherin, implicating an upstream effect of ERK1/2 on N-cadherin and also suggesting a link between Rab23 and ERK1/2. Further biochemical studies show that silencing of Rab23 impedes activation of ERK1/2 via perturbed platelet-derived growth factor-alpha (PDGFRα) signaling. Restoration of the expression of Rab23 or N-cadherin in Rab23-KD neurons could reverse neuron migration defects, indicating that Rab23 modulates migration through N-cadherin. These studies suggest that cortical neuron migration is mediated by a molecular hierarchy downstream of Rab23 via N-cadherin.

Key words: corticogenesis, ERK1/2, GTPase, N-cadherin, PDGFRα, Rab23, radial migration

Introduction

Cortical pyramidal/projection neurons originating from the ventricular layer are the neuronal type that forms the distinct multilayered cerebral cortex in mammals. During the onset of corticogenesis, newly born or radial glial progenitor cells in the ventricular zone (VZ) undergo asymmetric division to constitute a distinct basal/intermediate progenitor (IP) layer located basally above the VZ commonly term the subventricular zone (SVZ). These intermediate progenitors (mostly neurogenic) migrate radially through the intermediate zone (IZ) to terminally populate the entire apical–basal axis of the cortical plate where they differentiate and mature into cortical neurons (Rakic 1988; Bystron et al. 2008). Defective radial migration is known to cause numerous severe human neurological disorders and cortical malformations such as lissencephaly, polymicrogyria, schizencephaly, subcortical band hererotopia, schizophrenia, mental

retardation, and Alzheimer's disease (Kriegstein and Noctor 2004; Spalice et al. 2009; Valiente and Marín 2010; Geschwind and Rakic 2013).

Radially migrating projection neurons begin their journey from the apical aspect as bipolar neurons moving from the VZ to the neighboring subventricular zone (SVZ). Subsequently, they extend multiple processes and transiently changed into multipolar neuron as they transit into the intermediate zone (IZ). Prior to entering the cortical plate, the multipolar neurons retract their processes and switch back into bipolar shapes while adhering to radial glia fibers to initiate glial-guided locomotion into the cortical plate. In the final phase of radial migration, neurons translocate their cell bodies into the cortical plate (Nadarajah et al. 2001, 2003; Kriegstein and Noctor 2004; Stanco and Anton 2013).

To sustain the constantly transforming neuronal shape and polarity required by radial migration, it is necessary for neurons to constantly reorganize their cytoskeletal and cell adhesive properties (Bielas and Gleeson 2004; Moon and Wynshaw-Boris 2013). Failures to respond in step with the locomotory needs of neurons are known to occur in neurons carrying mutations of cytoskeletal-associated genes, such as β-tubulin subunit *TUBB2B*, lissencephaly 1 (*LIS1*), doublecortin (*Dcx*) and filamin 1 (*FLN1*) (Fox et al. 1998; Manent et al. 2009; Jaglin et al. 2009; Spalice et al. 2009; Moon and Wynshaw-Boris 2013). Likewise, cell adhesion proteins such as α3β1 integrin subunits and N-cadherin have been reported to be required for normal cortical neuronal migration in mouse models (Dulabon et al. 2000; Jossin and Cooper 2011; Shikanai et al. 2011)

Small GTPase are monomeric enzymes that can bind and hydrolyze guanosine triphosphate (GTP) with diverse cellular consequences during development. Notably Rho, Rnd, Arl13b, Arf, and Rab GTPases are important for controlling cell adhesion and cytoskeletal remodeling during neuronal migration (Azzarelli et al. 2014; Shah and Püschel 2014). Mechanistically, these small GTPases may govern the subcellular trafficking of cell adhesion molecules at the adhesive sites during migration (Kawauchi et al. 2010; Govek et al. 2011; Kawauchi 2011). In particular, certain endocytic Rabs such as Rab5, Rab11, and Rab7, have been shown to direct the endocytic trafficking, recycling and protein degradation of N-cadherin in the radially migrating projection neurons, which is required for orientated migration and radial-guided locomotion (Kawauchi et al. 2010; Jossin and Cooper 2011; Kawauchi 2012).

We are interested in Rab23 that is mainly localized to the plasma membrane and endosomes, and known to be expressed in the embryonic and adult brain (Olkkonen et al. 1994; Eggenschwiler et al. 2001; Guo et al. 2006). Specifically, Rab23 is highly enriched in the neurons as compared with astrocytes and oligodendrocytes (Guo et al. 2006). Despite its unknown function during neurogenesis, human patients recessive for *RAB23* suffer from Carpenter syndrome, with the subjects exhibiting varied degree of craniosynotosis, heart defect, multiple congenital malformations and other variable central nervous system (CNS)-related conditions including hydrocephaly, mental retardation and obesity (Jenkins et al. 2007, 2011; Hidestrand et al. 2009; Alessandri et al. 2010). In mice, *Rab23* null mutants have unclosed neural tubes and are embryonically lethal during the second-half of gestation (Eggenschwiler et al. 2001). Given these limitations of access, and its importance to human nervous system development, it is of interest to explore the mechanisms of Rab23 function during the development of the neocortex.

In this study, we used focused gene perturbation of Rab23 by in utero electroporation of cortical neurons, as well as tissue specific knockout of *Rab23* in the neocortex to study its function during cortical development. We show that Rab23 regulates the polarity and migration of projection neurons. Silencing of Rab23 resulted in the arrest of projection neuron migration in the apical ventricular/subventricular zone and intermediate zone by interfering the dynamics of cell polarity and cell shape changes necessary for the migration into the cortical plate. We provide evidence that these phenotypes are linked to Rab23-mediated control of N-cadherin expression. Moreover, the expression of N-cadherin in the cortical neurons is regulated via phosphorylation of ERK1/2 by PDGFRα. We suggest that Rab23 is an important player in the radial migration of cortical neurons by influencing the expression of N-cadherin during migration.

Results

Rab23 Regulates the Radial Migration of Cortical Neurons

The expression profile of Rab23 in the developing mouse cortex was examined by western blot analysis. This showed Rab23 expression throughout corticogenesis from E14.5 to the adult (12–20 weeks) (Fig. 1*a*). Interestingly, higher expression of Rab23 was detected in the adult compared with the juvenile stage (Fig. 1*a*). Immunostaining of the developing cerebral cortex revealed enriched Rab23 expression in the intermediate zone and cortical plate (CP) of E15 and E17 coronal brain sections, which are the regions where neurons reside (MAP2 positive neurons). In addition, Rab23 expression was lower in the proliferative regions of the VZ (Fig. 1*b*,*c*). Co-localizations of Rab23 with MAP2 (neuronal marker) and Nestin (radial glial marker) were observed at E15 (Fig. 1*c*), indicating the expression of Rab23 in neurons and radial glial cells. These expression profiles suggest a role for Rab23 functions in cortical neuronal development.

Rab23 null mutants are known to die in utero (Eggenschwiler et al. 2001), hence its roles in the later stages of cortical development remain unclear. To address this issue, we adopted a focused approach to knockdown Rab23 in the cortical neurons by in utero electroporation of shorthairpin RNA (shRNA) specifically targeting Rab23. shRab23 or control scrambled shRNA (shControl) expression vectors co-expressing EGFP were electroporated into E13 cerebral cortices when corticogenesis takes place. These electroporated cortices were harvested at E17, and EGFP-positive neurons were examined for perturbation effects. At E17, the majority of the shControl cortical neurons (~69%) revealed by EGFP resided in the cortical plate, whereas only about one-third (~34%) of the Rab23 knockdown (KD) group resided in the cortical plate. Correspondingly, ~20% and ~49% of the total shControl neurons and Rab23-KD neurons respectively were found in the intermediate zone (Fig. 2*a*,*b*). Another two shRNA sequences targeting different regions on Rab23 (shRab23_378 and shRab23_496) also resulted in similar positioning phenotype, showing excessive number of Rab23-KD cells positioning in the intermediate zone (Supplementary Fig. 1*a*,*b*). Overexpression of wild-type (WT) Rab23 (which transcripts are unaffected by the shRNA) together with shRab23 restored the positioning defects of Rab23-KD neurons (Fig. 2*a*,*b*). These data suggest that the shRab23-mediated positioning anomalies were due to the depletion of Rab23 proteins. Furthermore, examination of the E13-electroporated neurons at postnatal (P) day 21 revealed Rab23-KD neurons exhibiting sustained positioning defects (Fig. 2*e*).

The reduced proportion of EGFP-positive Rab23-KD neurons in the cortical plate, and the excessive accumulation of these EGFP-positive neurons in the intermediate zone imply defective

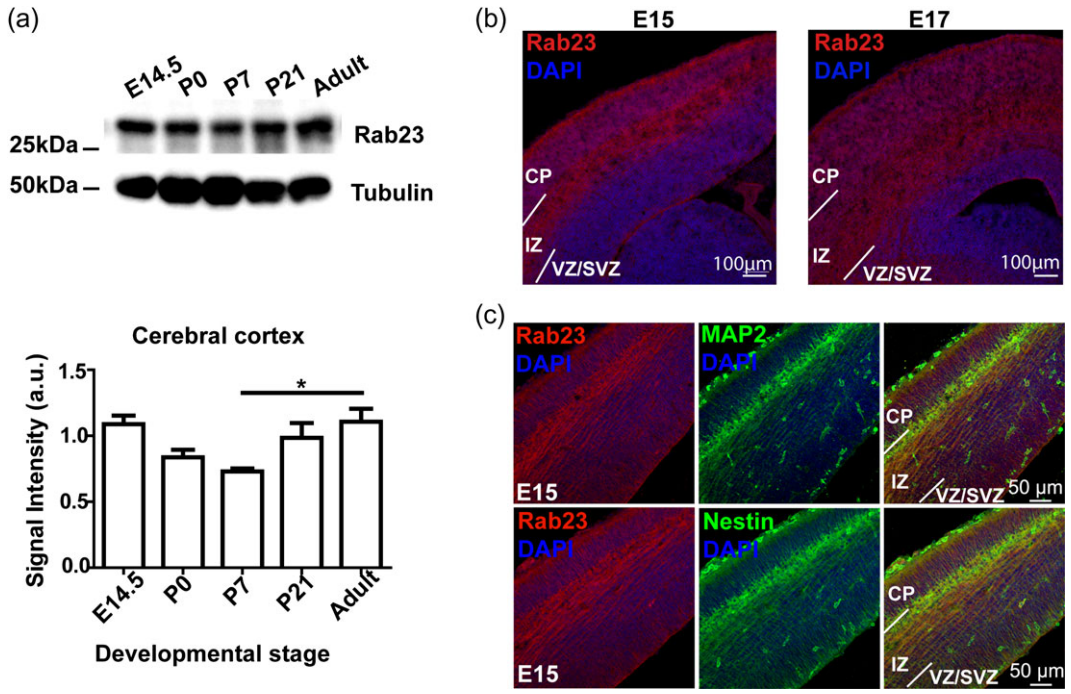

Figure 1. Rab23 is expressed in neurons and radial glial cells during mouse embryonic corticogenesis. (*a*) Western blot analysis of total protein lysate showed expression profile of Rab23 in the developing cerebral cortex. Rab23 expression persisted from embryonic stages to adulthood. (*b*) Immunostaining of Rab23 antibody on E15 and E17 cortical sections showed enrichment of Rab23 expression in the intermediate zone and cortical plate. (*c*) Co-immunostaining of Rab23 and neuronal marker, MAP2, or radial glial cells marker, Nestin showed positive expression of Rab23 in neurons and radial glial cells.

neuronal radial migration. The transition from a transient multipolar to a bipolar morphology is one of the crucial steps for cortical neurons to successfully migrate from the intermediate zone to the cortical plate (Kriegstein and Noctor 2004). To assess the consequences of Rab23 knockdown on neuronal morphology and polarity, we measured the proportions of neurons with unipolar, bipolar, multipolar and round (no visible polarity) morphologies. The majority (~60%) of the shControl neurons displayed unipolar or bipolar shapes (judged by the orientation of their processes). Interestingly, knockdown of Rab23 significantly reduced the percentage of uni/bipolar neurons (~40%) in the intermediate zone, but the percentage of multipolar neurons here was increased (~44%) compared with the shControl (~30%) group (Fig. 2*c*,*d*). These observations suggest that Rab23-KD neurons tend to assume multipolar morphologies in the intermediate zone.

Knockdown of Rab23 Does Not Affect Neuron Proliferation or Differentiation

To confirm that the aberrant accumulation of Rab23-KD neurons in the intermediate zone was a result of a migration defect, we examined other associated cellular processes including proliferation, differentiation and cell death. The proliferation profile of E13-electroporated cells expressing shControl or shRab23 was determined by intraperitoneal administration of 5′-ethynyl-2′-deoxyuridine (EdU) 2 h before fixing the brains at E15. Detection of EdU was performed 2 days after the introduction of shRab23 to ensure that the affected cells were still undergoing migration. Quantification of $EdU^+/EGFP^+$ cells showed that neither knockdown nor overexpression of wild-type Rab23 caused any change to the number of proliferating cells (Fig. 3*a*,*b*) suggesting that Rab23 does not regulate neuronal progenitor proliferation at this stage of corticogenesis. These observations are further supported by the cell cycle exit kinetics assessed by 24 h EdU long-pulse (from E14 to E15) assay. Double staining of Ki67 with EdU was performed to distinguish populations of cells exited ($Edu^+/Ki67^-$) or remained ($Edu^+/Ki67^+$) in the cell cycle. The comparable ratios of $EdU^+/Ki67^-/EGFP^+$ against all $EdU^+/EGFP^+$ cells in the knockdown and control groups indicated similar cell cycle exit kinetics between both groups (Fig. 3*c*,*d*). To rule out the possibility that decreased migration is a consequence of increased cell death, we examined the degree of neuronal apoptosis at E15 and E17 by immunostaining of cleaved-caspase 3 (CC3) and TUNEL assay. The percentage of $EGFP^+/CC3^+$ or $EGFP^+/TUNEL^+$ cells in shRab23-electroporated cortices is not significantly different from the shControl-electroporated cortices (Fig. 3*e*–*h*) at both time points, which suggests that Rab23 knockdown did not affect cell death and/or survival at this developmental stage.

To test if the abnormal positioning was a consequence of abnormal accumulation of progenitor cells, the numbers of shControl- or shRab23-expressing Pax6+ (radial glial cells) or Tbr2 + (intermediate progenitor cells) cells were counted. There were no significant differences in the numbers of progenitors in the knockdown group as compared with the control group (Fig. 3*i*,*j*). These data further confirmed that silencing of Rab23 causes migration or positioning anomalies without affecting progenitor cell proliferation or cell fate commitment. Next, differentiation of progenitors was examined by assessing the expressions of early and late neuronal differentiation markers, βIII-tubulin (Tuj1) and neuronal nuclei (NeuN). Rab23-KD cells were positive for these markers, suggesting a normal schedule of normal neuronal differentiation (Fig. 3*k*,*l*). These results suggest that the aberrant accumulation of Rab23-KD cells in the intermediate zone was not caused by abnormal neuronal differentiation.

Taken together, our data demonstrated an enhanced accumulation of Rab23-KD neurons in the intermediate zone, and

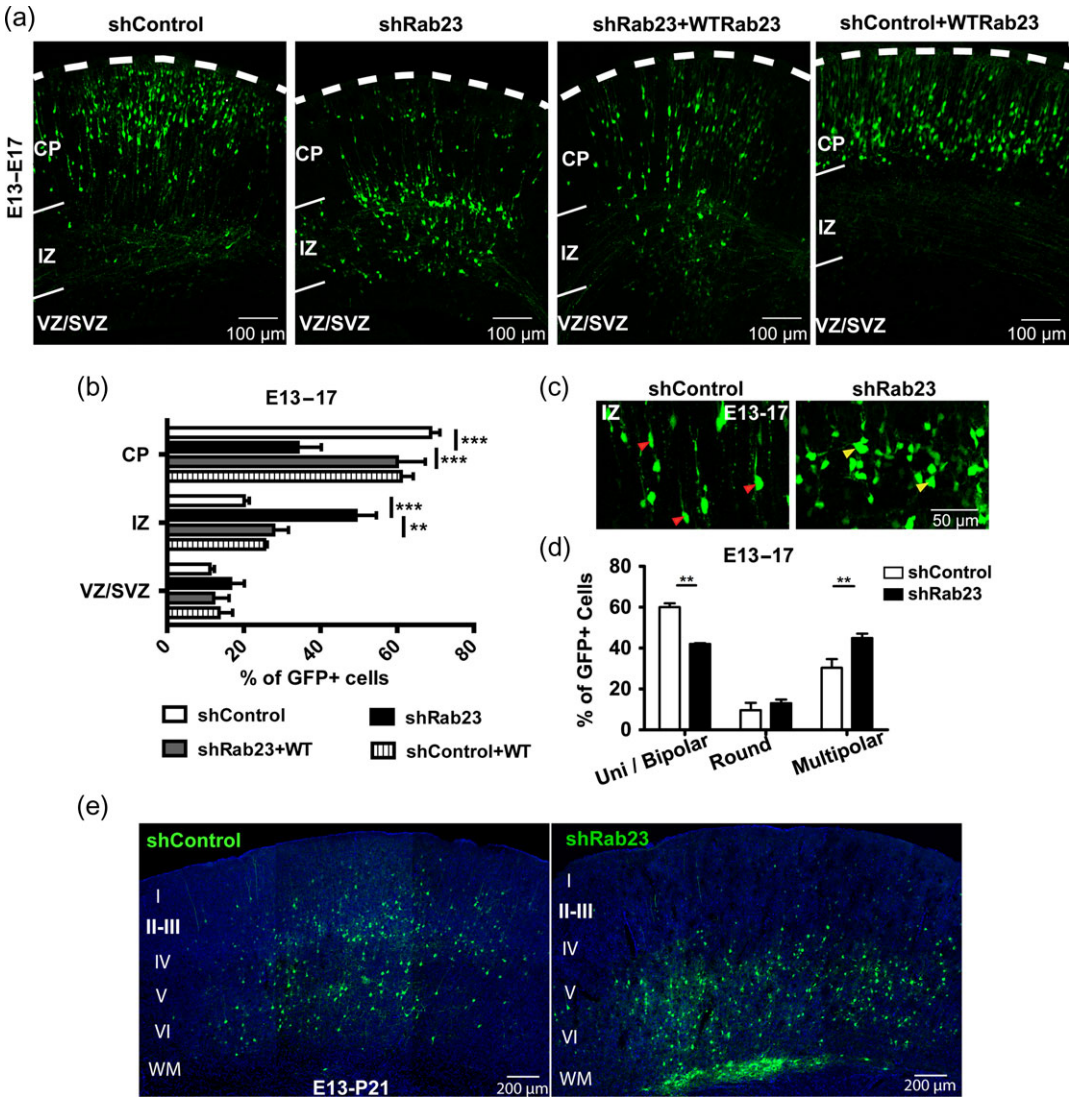

Figure 2. Knockdown of Rab23 causes ectopic accumulation of cortical neurons in the intermediate zone. (*a*) EGFP-tagged shControl, shRab23 and wild-type Rab23 overexpression constructs were in utero electroporated into the cerebral cortices of E13 mouse embryos respectively. EGFP-expressing neurons at E17 were visualized by immunostaining coronal sections of cortices with antibody recognizing EGFP. CP, cortical plate; IZ, intermediate zone; VZ, ventricular zone; SVZ, subventricular zone. (*b*) Percentage distribution of EGFP-positive neurons in each cortical layer was quantified and compared between different groups. The proportion of Rab23-KD neurons in the IZ was increased by two-fold compared with the control group. Co-expression of shRab23 and WTRab23 plasmids alleviated ectopic accumulation of EGPF-positive neurons in the IZ. n = 3–4 embryos; ~200–500 neurons were counted in each embryo; statistical values were determined by performing Two-way ANOVA Bonferroni's post-tests. *P value < 0.05; **P value < 0.01; ***P value < 0.001. (*c*) Polarity of the migrating neurons in the IZ was assessed by cellular morphological change. Neurons with 1–2 apical/basal projections and elongated in shape were categorized as uni/bipolar neurons (red arrowhead); without projection and round in shape were round neurons; with multiple projections and irregular shape were multipolar neurons (yellow arrowhead). (*d*) Rab23-KD neurons exhibited reduced proportion of uni/bipolar neurons and increased proportion of multipolar neurons as compared with the control counterpart. n = 3 embryos; ~50–100 neurons were counted in each embryo (statistical values were determined by performing Two-way ANOVA Bonferroni's post-tests **P value < 0.01). (*e*) Representative images showing the localization of shControl or shRab23-electroporated neurons at postnatal day 21 after prior electroporation at E13. n = 3 brains per group.

these neurons exhibited a lack of apical–basal polarity and the transition from a multipolar to a bipolar phenotype. However, the knockdown of Rab23 did not alter cell proliferation, differentiation, or cell death. These results suggest that the accumulation of Rab23-KD neurons in the intermediate zone was likely to result from impaired radial migration of projection neurons.

Rab23 Knockdown Neurons Exhibit Aberrant Migration Behaviors

Time-lapse imaging was performed on ex vivo cultured cortical slices to examine the migratory behaviors of cortical projection neurons. shControl or shRab23 constructs were electroporated ex utero into E14 cortical slices respectively. These brain slices were cultured for 2 days before being subjected to time-lapsed imaging analysis for 18 h to image radial migration of projection neurons from the intermediate zone to the cortical plate (Fig. 4*a*). Strikingly, Rab23-KD neurons failed to move to the cortical plate and were largely halted at the intermediate zone. Moreover, co-electroporation of WTRab23 with shRab23 could partially reverse the migration defects (Fig. 4*a*,*b*–*d*), suggesting that the phenotypes observed were due to a decrease in Rab23 protein. Rab23-KD neurons traveled shorter distances and exhibited reduced migration speed compared with that of control neurons

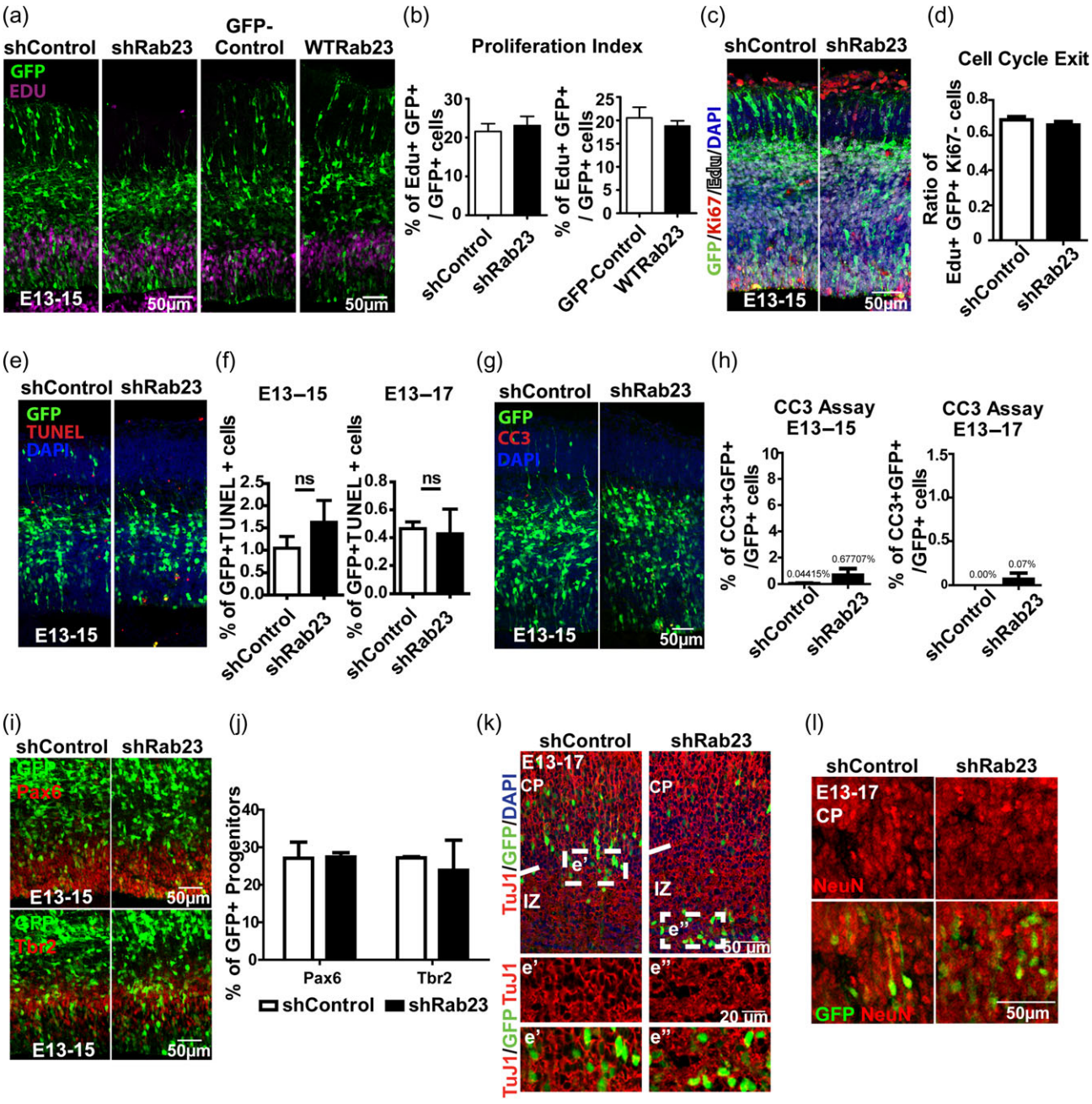

Figure 3. Knockdown of Rab23 does not alter cell proliferation, differentiation or cell death. (*a*) EdU was administered intraperitoneally into pregnant mice for 2 h at E15, 2 days after in utero electroporation. (*b*) Cell proliferation was assessed as the percentage of EdU/EGFP-positive cells against all EGFP-positive cells. Neither knockdown nor overexpression of wild-type Rab23 led to a change in the number of proliferative cells. $n = 3$ to 4 embryos; ~200–500 neurons were counted in each embryo. (*c*) Representative images showing co-staining of GFP/ki67/EdU on brain sections obtained from animals subjected to 24 h EdU-pulse from E14–15. (*d*) Cell cycle exit determined as the ratio of $EdU^+/EGFP^+/Ki67^-$ against all $EdU^+/EGFP^+$ cells. No change in the cell cycle exit was observed. (*e–h*) TUNEL (*e*) or CC3 (*g*) labelings were performed on brain sections of E15 and E17 embryos pre-electroporated at E13. Graphs showing (*f*,*h*) the percentages of cell death counted as the proportion of TUNEL/EGFP-positive or CC3/EGFP-positive cells against all EGFP-positive cells. No significant change in the amount of cell death was observed in the Rab23-KD brains. (*i*,*j*) Representative immunostaining images (*i*) and graphs showing quantification (*j*) of $Pax6^+/EGFP^+$ or $Tbr2^+/EGFP^+$ progenitors in the shControl or shRab23-electroporated brains sections. ns, not significant. $n = 4–5$ embryos; ~300 neurons were counted in each embryo. (*k*,*l*) Co-immunostaining of GFP with Tuj1 or NeuN antibodies showed that Rab23-KD neurons expressed Tuj1 and NeuN. Statistical values were determined by performing Student *t*-test.

(Fig. 4*f*,*g*). A trajectory/migration plot diagram illustrating the migration paths of the projection neurons show that the shControl neurons persistently migrated towards one direction (Fig. 4*b*,*h*). In contrast, Rab23-KD neurons showed inconsistent directions and random migration patterns (Fig. 4*c*,*h*). Overexpression of WTRab23 in the Rab23-KD neurons has modest, but statistically significant rescue effects on the distance, velocity and direction defects (Fig. 4*f–h*). Overexpression of WTRab23 with shControl resulted in comparable migration distance and velocity (Fig. 4*e–g*) but significantly perturbed directionality as compared with shControl (Fig. 4*h*). This implies a gain-of-function effect in the event of excessive expression of Rab23 in the projection neurons, which might explain the subtle recovery of directionality observed in the rescue group. These results reinforce our

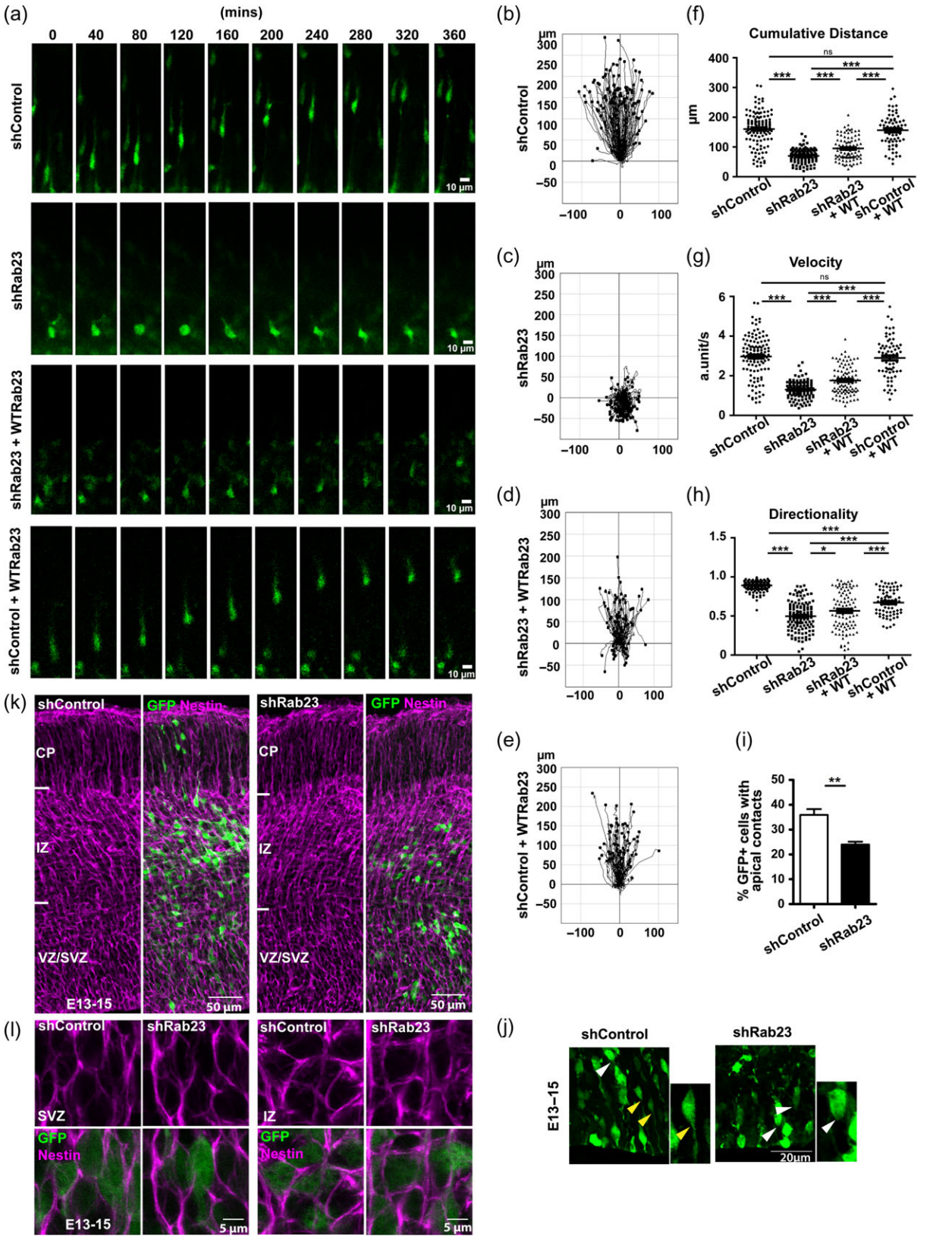

Figure 4. Rab23-KD neurons exhibit aberrant migration behaviors. (*a*) Representative time-lapse images of radially migrating neurons ex utero-electroporated with shControl, shRab23 and WTRab23 plasmids, respectively. (*b–e*) Trajectory/migration plots illustrate the migration paths of electroporated neurons entering CP from IZ. Each dot/line represents individual neuron. Number of neurons traced and analyzed; shControl = 125, shRab23 = 127, shRab23 + WTRab23 = 98, shControl + WTRab23 = 70. (*f*) Cumulative distance traveled by EGFP-positive neurons. (*g*) Migration velocity of EGFP-positive neurons. (*h*) Directional persistency of migration. Each dot represents individual neurons. Data were compiled from 3 independent experiments. Statistical values were determined by performing One-way ANOVA

initial observation with regards to the loss of apical–basal polarity in the Rab23-KD neurons. The loss of directed locomotion and perturbed migration of Rab23-KD projection neurons in the cerebral cortex is likely due to a failure to undergo multipolar–bipolar transition essential for establishing apical–basal polarity.

Indeed, we also observed a significantly reduced number of Rab23-KD neurons with apical projections as compared with control neurons (Fig. 4*i*,*j*). However, the morphological appearance of the radial glial scaffold in the Rab23-KD cortical slices did not exhibit any discernible defect as compared with the control counterpart (Fig. 4*k*,*l*). This lack of apical projections in Rab23-KD neurons indicates intrinsic destabilization of neuronal processes and possibly disrupted cytoskeletal reorganization process. Taken together, these results suggest that knockdown of Rab23 potentially perturbed the formation of neuronal processes and cell–cell interactions required for directed movement of projection neurons towards the cortical plate.

Rab23 Regulates the Expression of N-cadherin

As N-cadherin has been implicated in the modulation of cell adhesion during radial migration, we asked if N-cadherin expression or localization were affected in Rab23-KD neurons. N-cadherin expression in the in utero electroporated neurons was examined at protein level by immunohistochemistry, and at transcriptional level by quantitative (Q) PCR. Immunohistochemical staining revealed enriched N-cadherin expression at the plasma membrane of E15 neurons. The levels of N-cadherin at the plasma membrane located between two adjacent EGFP-positive neurons (blue arrowhead) were quantified and normalized to that of the plasma membrane adjacent to EGFP-negative neurons (yellow arrowhead). Strikingly, the expression of N-cadherin at the cell borders between two EGFP-positive neurons was profoundly reduced in the Rab23-KD group as compared with the shControl group (Fig. 5*a*–*c*), suggesting that Rab23 regulates the cell surface expression of N-cadherin in cortical projection neurons. QPCR analysis of the EGFP-enriched tissue regions similarly showed a reduction in *N-cadherin* mRNA expression in the Rab23-KD group (Fig. 5*d*).

Consistent with our data from cortical projection neurons in brain slices, the knockdown of Rab23 in cultured primary cortical neurons also significantly down-regulated N-cadherin expression (Fig. 5*e*–*i*, Supplementary Fig. 1*c*–*e*). The full-length (Fig. 5*f*,*g*) and the proteolytically cleaved form of N-cadherin's cytoplasmic fragment (CTF) (Fig. 5*f*,*h*) were both down-regulated in Rab23-KD neurons (Fig. 5*e*–*i*). To determine if the Rab23-KD-mediated decreased in N-cadherin expression occurs at the transcriptional level, mRNA extracts of DIV7 cortical neurons were harvested for QPCR assay (Fig. 5*j*). Knocking down of Rab23 in cultured cortical neurons resulted in a down-regulation of N-cadherin mRNA (Fig. 5*j*).

These results show that Rab23 KD affects mRNA and protein expression of N-cadherin in cultured neurons in vitro and in vivo in brain slices.

The Expression of N-cadherin is Influenced by PDGFRα-mediated Phosphorylation of ERK1/2

We further queried the underlying molecular mechanisms mediating N-cadherin expression. PDGFRα signaling was previously shown to modulate the N-cadherin-mediated mesodermal cell migration in chick embryo (Yang et al. 2008) and was also reported to promote the migration of oligodendrocyte progenitor cells by activating ERK1/2 signaling pathway (Frost et al. 2008). Furthermore, ERK1/2 was shown to mediate the expression of N-cadherin in schwannoma cells (Martiáñez et al. 2013). Therefore, we hypothesized that PDGFRα and/or ERK1/2 signaling pathways might be perturbed in Rab23-KD neurons, which consequently affected N-cadherin expression and neuron migration. To test the response of Rab23-KD neurons to PDGFRα signaling pathway, the PDGF-BB ligand (dimer of the B chain of human PDGF), which binds and activates PDGFRα receptor, was used to stimulate PDGFRα signaling activation in the control and Rab23-KD neurons. Control neurons treated with PDGF-BB triggered markedly increased activation of PDGFRα signaling, as showed by an average of 8 times up-regulation of tyrosine-phosphorylation of PDGFRα (Fig. 6*a*,*b*). PDGF-BB treatment in control neurons also increased the phosphorylation of ERK1/2, by about 4 times (Fig. 6*c*,*d*). However, PDGF-BB-stimulated phosphorylation of PDGFRα (2.5 times) and ERK1/2 (2.5 times) were significantly lower in the Rab23-KD neurons as compared with the control neurons (Fig. 6*a*–*d*). These data indicate that Rab23 is required for the activation of PDGFRα signaling cascade demonstrated by the phosphorylation of PDGFRα and ERK1/2 in the cortical neurons.

Consistent with these data is our observation that knocking down of Rab23 decreased phosphorylation of ERK1/2 (Fig. 6*e*,*f*). Inhibiting the phosphorylation of ERK1/2 by PD98059 or U0126 decreased N-cadherin expression (Fig. 6*g*,*h*). However, N-cadherin-KD did not alter the phosphorylation level of ERK1/2 (Fig. 6*i*,*j*). Taken together, these results suggest Rab23 regulates N-cadherin expression by positively mediating PDGFRα-dependent phosphorylation of ERK1/2.

N-cadherin Expression is Critical for Rab23-mediated Cortical Migration

To determine if the reduction of N-cadherin expression level underlies the Rab23-KD-induced migration defects, WT-N-cadherin expression construct was co-electroporated with shRab23 construct in utero. Expression of WT-N-cadherin in Rab23-KD neurons significantly increased the percentage of projection neurons reaching the cortical plate as compared with the population of shRab23 knockdown neurons. In addition, the percentage of neurons that were accumulated in the intermediate zone was significantly reduced as compared with the Rab23-KD population (Fig. 7*a*,*b*). To further confirm the recovery of migration defects in Rab23-KD neurons, ex vivo cortical slice cultures were imaged at real-time to follow the migration behaviors of EGFP-positive neurons (Fig. 7*c*). Detailed time-lapse analysis showed that expression of WT-N-cadherin in the Rab23-KD neurons could rescue the Rab23-KD-dependent migration distance (Fig. 7*d*,*f*,*h*) and velocity (Fig. 7*i*) but did not show significant improvement in the migration directions (Fig. 7*j*). Overexpression of WT-N-cadherin alone resulted in disrupted migration directionality, but these cells showed migration distance and velocity that are similar to the shControl expressing neurons (Fig. 7*d*–*j*). Furthermore, assessment of the cell polarity of cells in the intermediate zone similarly revealed that co-expression of N-cadherin in the

Bonferroni's multiple comparison test. (*i*,*j*) Most Rab23-KD neurons in the VZ lack apical contacts. Yellow arrowhead: neurons with apical projections/contacts; white arrowhead: neurons without apical projections/contacts. $n = 3$ embryos; ~100 neurons were counted in each embryo. (*k*,*l*) Representative images of brain sections electroporated with shControl or shRab23 constructs, illustrating the morphology of radial glial scaffold via Nestin immunostaining. (*l*) Close up images of radial glial scaffold in the SVZ (left panel) and IZ (right panel). CP, cortical plate; IZ, intermediate zone; VZ, ventricular zone; SVZ, subventricular zone. Statistical values were determined by performing Student *t*-test. *P value < 0.05; **P value < 0.01; ***P value < 0.001.

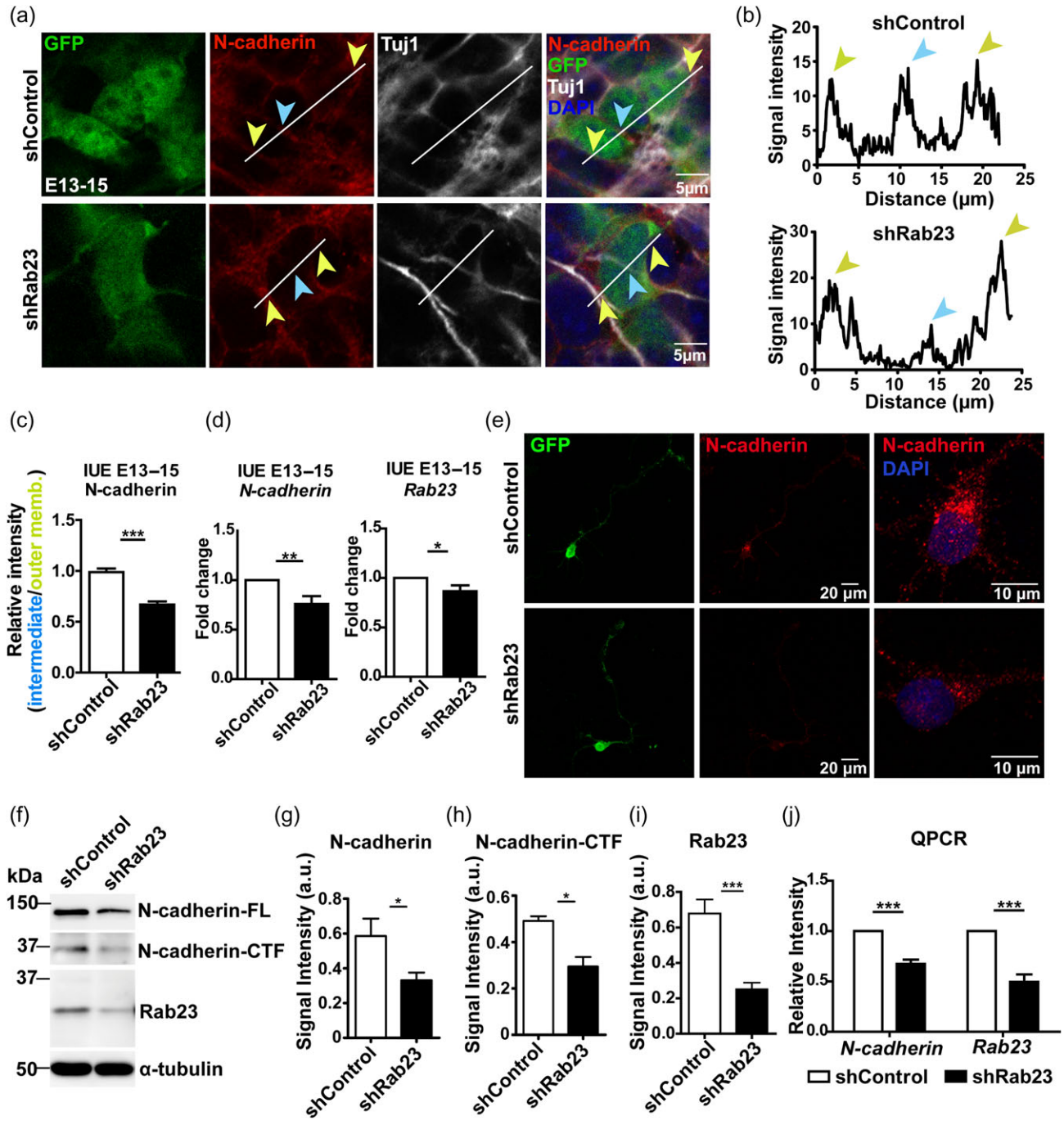

Figure 5. Rab23 regulates N-cadherin expression in the cortical neurons in vivo and in vitro. (*a*) Representative immunostaining images of N-cadherin and TuJ1 on E13-15 electroporated cortical tissue sections. (*b*) Representative expression profile of N-cadherin measured across the cell bodies of pairing EGFP-positive neurons. (*c*) Expression levels of N-cadherin at the intermediate cell membrane/border (blue arrowheads) of two pairing EGFP-positive neurons were quantified against its respective outer membranes (yellow arrowheads). For each pairing groups, average highest peak values of its respective intermediate or outer cell borders were obtained from 3 proximal parallel lines drew across the cell bodies of pairing neurons. Number of pairing neurons analyzed; shControl = 38, shRab23 = 36. Data were compiled from 3 independent biological repeats. Statistical values were determined by performing Student *t-test*. ***P value<0.001. (*d*) Graphs showing QPCR quantification of *N-cadherin* and *Rab23* expression in the E13-15 IUE brains. Data represents 5 biological repeats for each group. (*e*) Representative images demonstrating expression and localization of N-cadherin in shControl or shRab23-expressing primary cortical neurons. (*f–i*) Representative western blots (*f*) showing expression and graphs (*g–i*) showing quantification of Rab23, N-cadherin FL and CTF upon knocking down Rab23 in primary cortical neurons. α-tubulin was used as the loading/normalization control. (*j*) Graph illustrates knocking down of Rab23 in primary cortical neurons decreases mRNA level of *N-cadherin* as assessed by QPCR analysis. The readouts of *Rab23* and *N-cadherin* were normalized to *Gapdh* (reference gene). Quantifications represent 5 independent sets of samples. Statistical values were determined by performing Student *t*-test. *P value < 0.05; **P value < 0.01; *** *P* value < 0.001.

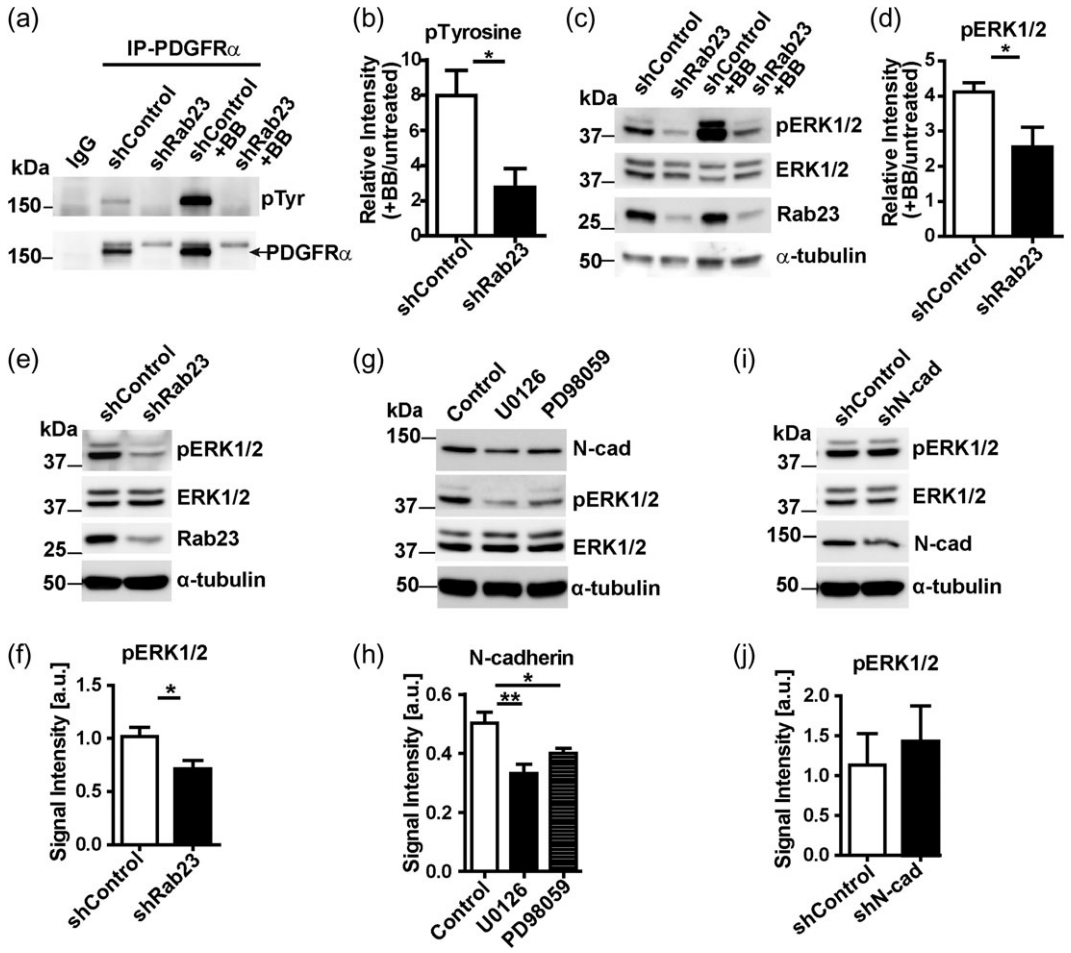

Figure 6. Rab23 regulates the expression of N-cadherin through PDGFRα-mediated phosphorylation of p44/42 ERK. (*a*, *b*) Representative western blot (*a*) and quantification analysis (*b*) showing immunoprecipitation assay detecting tyrosine phosphorylation levels of PDGFRα in shControl or shRab23 expressing neurons stimulated with vehicle or PDGF-BB. Graph illustrates PDGF-BB-stimulated expression levels of phosphor-tyrosine in shControl or shRab23 normalized to the phosphor-tyrosine of its respective untreated group. (*c*,*d*) Representative western blot (*c*) and quantification analysis (*d*) showing protein levels of phosphor-ERK1/2, total ERK1/2 and Rab23 in neurons expressing shRab23 or shControl stimulated with vehicle or PDGF-BB. Graph illustrates PDGF-BB-stimulated expression levels of phosphor-ERK1/2 in shControl or shRab23 normalized to the phosphor-ERK1/2 of its respective untreated group. (*e*,*f*) Representative western blot (*e*) and quantification analysis (*f*) showing protein levels of phosphor-ERK1/2, total ERK1/2 and Rab23 in cells expressing shRab23 or shControl. (*g*,*h*) Representative western blot (*g*) and quantification analysis (*h*) showing protein levels of phosphor-ERK1/2, total ERK1/2 and N-cadherin in neurons treated with ERK inhibitors, U0126 (50 μM) or PD98059 (25 μM). (*i*,*j*) Representative western blot (*i*) and quantification analysis (*j*) showing protein levels of phosphor-ERK1/2, total ERK1/2 and N-cadherin in cells expressing shN-cadherin or shControl. For the western blot images of phosphor-ERK and total ERK, upper bands illustrate phosphor- or total ERK1 and lower bands illustrate phosphor- or total ERK2 respectively. Quantifications of phosphor-ERK1/2 were normalized to total ERK1/2 and α-tubulin. Quantification of tyrosine-phosphorylated PDGFRα was normalized to total PDGFRα and α-tubulin. Quantification analyses were compiled from 4 to 5 independent experiments. α-tubulin was used as the loading/normalization control. Statistical values were determined by performing Student *t*-test for comparison between 2 sample groups, and One-way ANOVA, Newman–Keuls multiple comparison test for comparison between 3 groups of samples *P value < 0.05; **P value < 0.01; ***P value < 0.001.

Rab23-KD neurons did not increase the number of uni/bipolar cells as compared with the knockdown group (Fig. 7*k*). These data suggest that N-cadherin overexpression could not restore the polarity and the direction of migration.

Knockout of Rab23 in EMX1-specific Cells Affects Neuron Migration and N-cadherin Expression

To investigate the role of Rab23 in early brain development, *Rab23* deletion was initiated in the telencephalon of the neocortex at ~E10.5. Mouse carrying *Rab23*-floxed homozygous allele was crossed with Emx1-Cre (Gorski et al. 2002), Radially migrating neurons were labeled by in-utero electroporation of EGFP expression vector into the neurons at E13. The migration profile of EGFP-expression neurons was examined 4 days later at E17 (Fig. 8*a*). In line with the earlier observation in Rab23-KD neurons, Rab23-conditional knockout (CKO) neurons also exhibited, albeit more moderate, radial migration defects. Approximately 80% of the EGFP-positive neurons in the control animal have reached the cortical plate at E17. Whereas only ~60% of the Rab23-deficient neurons have reached the cortical plate at the same time point. There were greater proportions of Rab23-CKO neurons residing in the intermediate zone, subventricular and ventricular zone, as compared with those in the control animal (Fig. 8*b*). Furthermore, the Rab23-CKO neurons also exhibited aberrant morphology and more multipolar as compared with the control counterparts at E17 (Fig. 8*c*). Moreover, the expression of N-cadherin in the cortical tissue extracts of the Rab23-CKO animals was lower than that of the control animals (Fig. 8*d*–*f*). No significant changes in the phosphorylation levels of PDGFRα and ERK were observed in the Rab23-CKO as compared with the control animals (Fig. 8*g*–*j*). These data demonstrate that in vivo knockout of *Rab23* in the neocortex bears

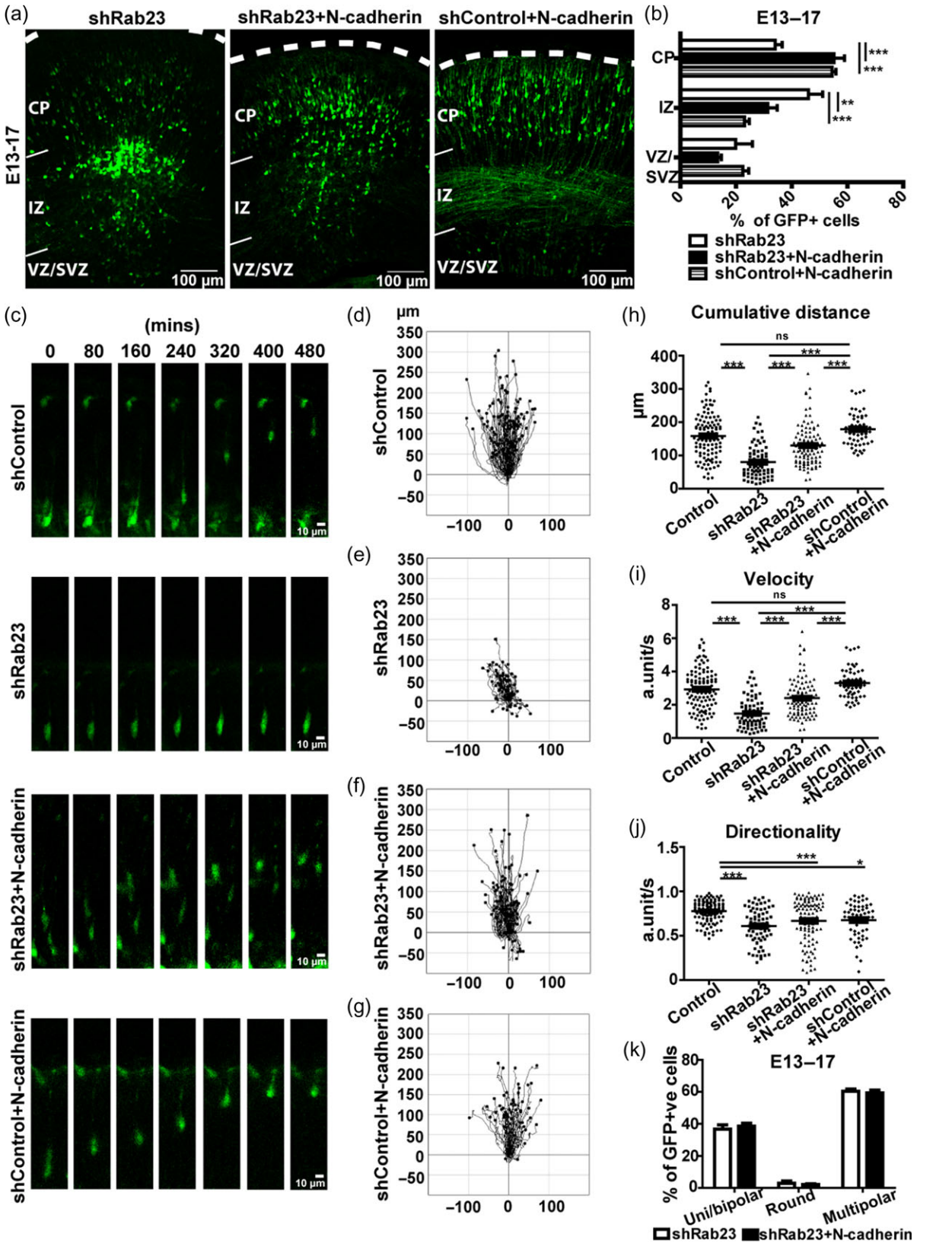

Figure 7. Restoration of N-cadherin expression alleviates the migration defects of Rab23-KD neurons. (*a*) N-cadherin expression was restored by in utero co-electroporation of EGFP-tagged shRab23 and wild-type N-cadherin overexpression constructs into the cerebral cortices of E13 mouse embryos. EGFP-expressing neurons at E17 were visualized by immunostaining of GFP antibody on coronal sections of cortices. CP, cortical plate; IZ, intermediate zone; VZ, ventricular zone; SVZ, subventricular zone. (*b*) Percentage distribution of EGFP-positive neurons in each cortical layer was quantified and compared between different groups. The proportion of neurons co-expressing Rab23-KD and wild-type N-cadherin overexpression plasmids in the CP was significantly increased compared with the Rab23-KD group.

resemblance to that observed in Rab23-KD neurons, and resulted in aberrant radial migration and N-cadherin expression.

It is worth noting that there is a discrepancy between the degree of Rab23 loss and N-cadherin loss in the Rab23-KD and conditional-KO models. Emx1 driven Rab23-CKO resulted in a more global depletion of Rab23, but only a moderate reduction of N-cadherin and consequently a more modest radial migration defect. The severity of the migration defect phenotype is therefore proportionate to the loss of N-cadherin, rather than Rab23. We do not yet have a robust explanation as to why Rab23-KD in utero at E13 should reduce N-cadherin more severely compare to Rab23-CKO in vivo from ~E10.5. However, it is plausible that compensatory mechanisms, acting from an earlier time point and for a longer period (~E10.5–E17 vs. E13–E17) may have sustained or restored N-cadherin levels despite the loss of Rab23.

Discussion

Radial migration of projection neurons during corticogenesis is a key step for the formation of distinct layers of cortical neurons in the mammalian cerebral cortex. Our findings uncovered a novel function of Rab23 in radial migration of projection neurons from the apical progenitor zones to the cortical plate. Emx1-Cre driven tissue-specific conditional knockout of *Rab23*, as well as in utero knockdown of Rab23 in the neocortex perturbed radial migration, as observed at E17. Rab23-KD neurons displayed restricted radial movements and were predominantly stalled in the intermediate zone resulting in an expanded population of these neurons accumulating in the intermediate zone correlating with the reduced number in the cortical plate.

During cortical migration, dynamic microtubule and/or actin cytoskeletal remodeling underlie cellular morphological changes for the initiation of cell–cell adhesion and neuronal processes formation (Valdeolmillos and Moya 2013). Our data showed that knockdown of Rab23 perturbed multipolar–bipolar transition of radially migrating neurons. This result suggests a role for Rab23 in mediating cell adhesion and cytoskeleton reorganization dynamics during the process of neuronal migration. Other Rab GTPases, including Rab5, Rab7, Rab11, and Rab21, have been reported to function in the cell adhesion and migration regulatory machinery (Pellinen et al. 2006; Kawauchi et al. 2010). Notably, Rab5, Rab7, and Rab11 were reported to orchestrate cortical migration via endocytosis-mediated membrane trafficking of N-cadherin, a key mediator of cell adhesion during migration (Kawauchi et al. 2010; Shih and Yamada 2012).

In this study, we found that Rab23 functions as another essential upstream modulator of N-cadherin during cortical neuronal migration. Both in vivo knockout and in utero knockdown of Rab23 in the neocortex resulted in reduced expression of N-cadherin. This reduction in N-cadherin potentially affected cell adhesion steps essential for directional cell migration. Furthermore, knockdown of Rab23 in primary cortical neurons also resulted in a significant reduction of N-cadherin proteins, including both the full-length and proteolytically cleaved cytoplasmic fragments of N-cadherin. The cytoplasmic fragment was previously reported as a constitutive and activity inducible product of N-cadherin shedding, which is generated by a sequential ADAM10 and Ps-1/γ-secretase complex-mediated proteolytic cleavage (Uemura et al. 2006). Furthermore, ADAM10 stimulated cleavage of N-cadherin was documented to promote cell–cell adhesion and migration, although the underlying mechanism of action is not clearly characterized (Reiss et al. 2005; Kohutek et al. 2009). Given that both full-length and truncated cytoplasmic fragment of N-cadherin positively stimulate cell adhesion and migration, it is likely that the down-regulation of N-cadherin underlies the radial migration defects found in Rab23-deficient neurons. N-cadherin was previously reported to regulate cell–cell adhesion and the polarity of migrating neurons for their radially directed migration in the cerebral cortex (Jossin and Cooper 2011; Shikanai et al. 2011). In our study, knocking down of Rab23 likewise disrupted directional movement and neuronal projections, indicating a loss of polarity and impaired cell adhesion critical for migration.

Co-expressing N-cadherin in the Rab23-KD neurons successfully rescued the radial migration defects, inferring that Rab23 was acting through N-cadherin to coordinate cortical radial migration. However, it is notable that the defective polarity or directional movement was not rescued by the co-expression of N-cadherin. This could potentially due to the gain-of-function phenotype upon N-cadherin overexpression, which resulted in impaired directionality. In addition, this could also be attributed to the technical difficulty in achieving optimal N-cadherin expression levels for proper migration. As shown previously, both up-regulation and/or down-regulation of N-cadherin expression would lead to impaired cortical radial migration (Shikanai et al. 2011). Indeed, we performed immunostaining of N-cadherin in the shRab23 and WT-N-cadherin co-electroporated brain sections and observed that neurons bearing highest expression level of N-cadherin tend to be halted at the intermediate zone (data not shown). It is also possible that other unknown downstream factors of Rab23 are also important in modulating the polarity and/or directional movement of projection neurons. At the very least, our results showed that N-cadherin is a key downstream factor of Rab23 required for cortical radial migration.

Previous studies have implicated Rab GTPases such as Rab5, Rab7, and Rab11 in regulating the endocytosis, recycling, and lysosomal-dependent degradation of N-cadherin in the cortical neuron respectively (Kawauchi et al. 2010). As part of the Rab GTPases family of membrane trafficking proteins, Rab23 has been shown to localize at the plasma membrane and various endocytic vesicles in a kidney fibroblast cell line (Evans et al. 2003). However, Rab23 has not been demonstrated to function in endocytosis in all cell lines studied so far, including HeLA, A431 and mesangial cells (Guo et al. 2006; Huang et al. 2011). We showed that knockdown of Rab23 caused a reduction of N-cadherin levels at the plasma membrane in vivo, but this reduction is correlated with a general reduction in its protein levels in the cell. No change was observed in the rate of transferrin endocytosis in Rab23-knockdown primary neurons (data not shown), suggesting a lack of function in neuronal endocytosis. Thus, Rab23 is not likely to regulate N-cadherin via endocytosis. Interestingly, the decrease in N-cadherin expression occurred at the transcription level as there was also a reduction in *N-cadherin* mRNA in the Rab23-KD cells. This change in mRNA level could potentially be attributed to the modulation of mRNA transcription and stability.

$n = 3$ embryos; ~200–500 neurons were counted in each embryo (statistical values were determined by performing Two-way ANOVA Bonferroni's post-tests *P value < 0.05; **P value < 0.01; ***P value < 0.001) (*c*) Representative time-lapse images of radially migrating neurons ex utero-electroporated with shControl, shRab23 and shRab23+WT-N-cadherin plasmids respectively. (*d–f*) Trajectory/migration plots illustrate the migration paths of electroporated neurons entering CP from IZ. (*g*) Cumulative distance traveled by EGFP-positive neurons. (*h*) Migration velocity of EGFP-positive neurons. (*i*). Directional persistency of migration. Each dot/line represents individual neuron. Number of neurons traced and analyzed from 3 independent experiments; shControl = 112, shRab23 = 72, shRab23 + WT-N-cadherin = 102 shControl + N-cadherin = 56. Statistical values were determined by performing One-way ANOVA Bonferroni's multiple comparison test. ***P value < 0.001.

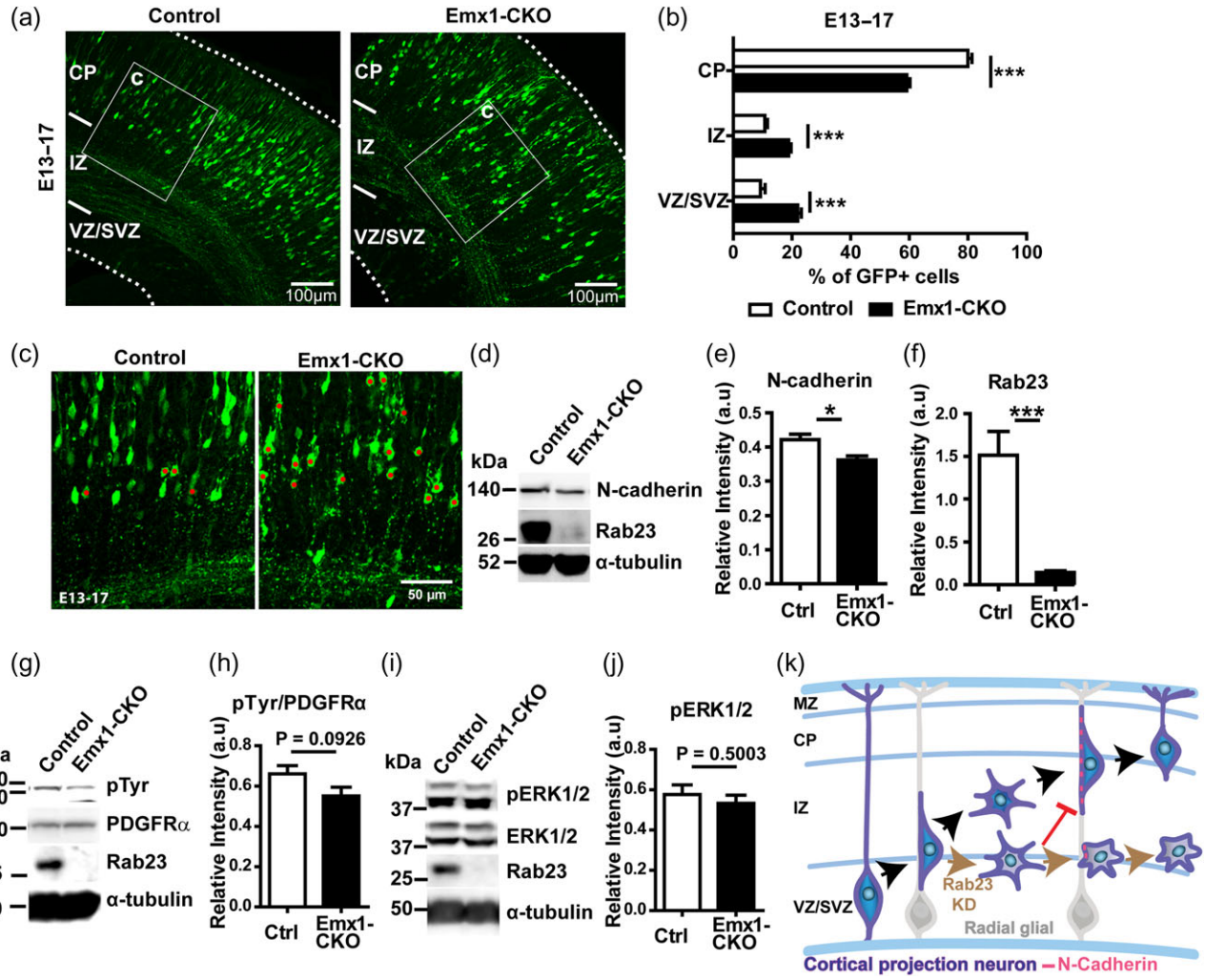

Figure 8. *Emx1-Cre* driven conditional knockout of *Rab23* in the cerebral cortex causes migration defect and reduces expression of N-cadherin. (*a*) EGFP-expressing vector was in utero electroporated into the cerebral cortices of E13 control and Rab23-CKO mouse embryos respectively to label the migrating neurons. EGFP-expressing neurons at E17 were visualized by immunostaining coronal sections of cortices with antibody recognizing EGFP. CP, cortical plate; IZ, intermediate zone; VZ, ventricular zone; SVZ, subventricular zone. (*b*) Percentage distribution of EGFP-positive neurons in each cortical layer was quantified and compared between different groups. The proportion of Rab23-KO neurons in the VZ/SVZ was increased by two-fold compared with the control group. $n = 4$ embryos per group; ~200–500 neurons were counted in each embryo (statistical values were determined by performing Two-way ANOVA Bonferroni's post-tests. ***P value < 0.001). (*c*) Representative close up images show higher number of neurons bearing aberrant polarity/morphology (labeled red dot) in the Rab23-CKO group. (*d–f*) Representative western blot (*d*) and quantification analysis (*e,f*) showing protein levels of N-cadherin and Rab23 in the cerebral cortex of control ($n = 7$) and Rab23-CKO mutant ($n = 6$) respectively. (*g,h*) Representative western blot (*g*) and quantification analysis (*h*) showing protein levels of pTyrosine and PDGFRα in the cerebral cortex of control ($n = 6$) and Rab23-CKO mutant ($n = 6$) (i,j) Representative western blot (i) and quantification analysis (j) showing protein levels of pERK1/2 and total ERK1/2 in the cerebral cortex of control ($n = 6$) and Rab23-CKO mutant ($n = 6$). For the western blot images of phosphor-ERK and total ERK, upper bands illustrate phosphor- or total ERK1 and lower bands illustrate phosphor- or total ERK2 respectively. Quantifications of phosphor-ERK1/2 were normalized to total ERK1/2 and α-tubulin. Quantification of phosphor-tyrosine was normalized to total PDGFRα and α-tubulin. α-tubulin was used as the loading/normalization control (statistical values were determined by performing Student *t-test*. *P value < 0.05; ***P value < 0.001). (*k*) Model illustrates silencing of Rab23 in cortical projection neurons affects N-cadherin expression resulting in altered migration of neurons through cortical layers. MZ, Mantle zone; CP, cortical plate; IZ, intermediate zone; VZ, ventricular zone; SVZ, subventricular zone.

Hence, the degradation kinetic of *N-cadherin* mRNA transcripts will require further investigations. On the other hand, we showed the transcriptional regulation of Rab23 on *N-cadherin*, which is likely to be indirect, i.e., through signaling pathways that influence the transcription of *N-cadherin*.

PDGFRα and ERK1/2 signaling pathways were reported to affect N-cadherin expression and cell migration in oligodendrocyte progenitor cells and mesoderm cells (Frost et al. 2008; Yang et al. 2008). In line with these findings, we found that knockdown of Rab23 down-regulated the phosphorylation of PDGFRα and ERK1/2 in primary cortical neurons. Furthermore, pharmacological inhibition of ERK1/2 activity in cortical neurons reduced N-cadherin expression, indicating an ERK1/2-dependent modulation of N-cadherin expression. Previous studies in hippocampal neurons and glioma stem cells have reported the influence of N-cadherin on ERK phosphorylation (Schrick et al. 2007; Velpula et al. 2012). However, we did not observe a discernable change in the phosphorylation level of ERK upon knocking down of N-cadherin in the cortical neurons, implying that the reduction in N-cadherin that we observed here is downstream of ERK1/2 activation. These data suggest that Rab23 positively influences N-cadherin expression in the cortical neurons, via ERK1/2 signaling. Recent study has reported that Rab23 is involved in the ciliary transport (Lim and Tang 2015) of membrane receptors to the

cilia, such as G-protein coupled receptors (GPCRs) (Leaf and Von Zastrow 2015), which potentially influences the membrane receptor-dependent downstream signaling cascade, such as ERK1/2 signaling pathway. Notably, PDGF receptor-alpha, a receptor tyrosine kinase, was found to stimulate ERK1/2 phosphorylation via primary cilia in fibroblast cells (Schneider et al. 2005). Therefore, we speculated that Rab23 affects ERK phosphorylation through PDGF membrane receptor signaling. Indeed, our data demonstrated that knockdown of Rab23 in the cortical neurons significantly suppressed the expression and activation of PDGFRα, thereby impeding the phosphorylation of ERK1/2. These data demonstrate a novel function of Rab23 in facilitating the signal transduction of PDGFRα to promote the activation of ERK1/2 and subsequently modulates the expression of N-cadherin.

Taken together, our findings shed light on the physiological and cellular functions of Rab23 in mammalian corticogenesis, beyond the point of embryonic lethality caused by its null allele. We demonstrated that Rab23 is required to ensure proper polarity and migration of projection neurons in the developing cerebral cortex (Fig. 8*k*). N-cadherin plays important roles in neuronal migration and is up-regulated by Rab23 at the transcription level. This is unlike other known Rab proteins that control N-cadherin surface expression and function through regulating its endocytic trafficking. This data opens up a new dimension in the roles played by Rabs during cortex development. To summarize, we show Rab23 regulates N-cadherin-mediated cell polarity and migration of cortical projection neurons during the development of cerebral cortex.

Methods

Animals

Rab23-floxed aminal was generated by Ozgene Pty Ltd. Conditional *Rab23-floxed* allele was designed by flanking exon 4 for *Rab23* gene with loxP sites. Emx1-Cre was purchased from Jackson Laboratory (cat no. 005 628). Control animals for conditional knockout experiments were animals either homozygous or heterozygous for *Rab23-floxed* allele. Rab23-CKO mutants used for all analyses were homozygous for *Rab23-floxed* allele and heterozygous for *Emx1-Cre* allele. All animals were housed in Specific Pathogen Free (SPF) animal facility at Duke-NUS Medical School, Singapore. All animal related procedures were carried out in compliance to animal handling guidelines and protocol approved by IACUC Singhealth, Singapore.

Expression Vectors

For in utero electroporation and in vitro viral transduction assay, Rab23 overexpression or knockdown sequences were cloned into retroviral pUEG or lentiviral pFUGW backbone respectively. For knockdown of Rab23, short-hairpin (sh) RNA sequence targeting sense sequence of 3′ UTR of Rab23 was 5′-GGACATACTTTACAGAAAG-3′ (mouse), 5′-AGACATACTCTACAGAACG-3′ (rat). shRab23_378 and shRab23_496 target mouse/rat Rab23 coding region were 5′-GGATGATTCATGCATCAAA-3′ and 5′-GCTGAGAAACACCTACAAA-3′ respectively. Scramble sh control sequence was 5′-AGTTCCAGTACGGCTCCAA-3′. U6 promoter was used to drive sh expression. EGFP sequences was inserted downstream of sh sequence under the control of Ubc promoter. For wild-type (WT) Rab23 overexpression construct, previously described full-length Rab23 sequence (Guo et al. 2006) was sub-cloned into pUEG or pFUGW vector driven by Ubc promoter. Wild-type N-cadherin construct was a kind gift from Kawauchi T and Richard L. Huganir and shN-cadherin was shNC-1023 from Kawauchi T. (Kawauchi et al. 2010). All plasmids were amplified according to the recommended protocol using Endofree® plasmid purification kit (Qiagen, Germany).

Viral Transduction and Culturing of Primary Rat Cortical Neurons

For viral transduction of primary cortical neurons, self-inactivating murine lentiviruses were prepared according to the previously described protocol (Ng et al. 2013). E18 rat cortical neurons were harvested and dissociated as described previously (Goh et al. 2008; Su et al. 2015). Dissociated neurons were plated on poly-L-lysine coated culture plates at the desired cell densities in MEM (Gibco®, Life Technologies, USA) medium containing horse serum, N2 supplement, sodium pyruvate (1 mM), glucose (0.2 M) and cytosine arabinoside (5 μM). Viral transduction was performed a day after culture while replacing the culture medium to maintenance medium consisting of Neurobasal (Gibco®, Life Technologies, USA), B27, L-glutamine and penicillin/streptomycin. The efficiencies of lentiviral vectors were validated by western blot analysis in neurons at DIV7.

pERK Inhibitors Assay

Primary cortical neurons were seeded in 6 well plates at a cell density of 2 million cells per well, and incubated in media containing 25 μM PD98059 (Cell Signaling Technology #9900) or 50 μM U0126 (Sigma-Aldrich #U120) from DIV 1 in maintenance medium. Equal volume of DMSO was added in a separate well for vehicle control. Media were replaced with fresh media with drugs or with DMSO on DIV 3. Total protein lysates were harvested on DIV 5 for SDS-PAGE and western-blot analysis.

PDGF-BB Stimulation Assay

DIV 7 cortical neuron culture was incubated with 50 ng/mL of PDGF-BB (Thermo Scientific, #PHG0045) for 10 min at 37 °C. Total protein lysates were extracted immediately after the PDGF-BB stimulation. Equal amount of lysates were heat denatured and subjected to western blot assay for the assessment of pERK1/2 expression. Another portion of the lysates was subjected to immunoprecipitation for the assessment of PDGFRα activation.

Immunoprecipitation

Total protein lysates of DIV7 cortical neurons were used for immunoprecipitation. Anti-PDGFRα antibody (Santa Cruz, #SC338) was incubated with 600 μg of protein lysates for each sample at 4 °C overnight. To isolate the antigen–antibody complex, immobilized protein A/G resin beads (Thermo Scientific, #53 132) were added to the antigen–antibody mixture and incubated at room temperature for 2 h. The immunogen complex bound to the A/G resin beads were collected by centrifugation, followed by several washes in IP buffer (25 mM Tris, 150 mM NaCl, pH 7.2). Immunogen complexes were then subjected to heat-denaturation at 100 °C, SDS-PAGE and western blot for the detection of phosphorylated-PDGFRα.

Ex-vivo Electroporation and Cortical Slice Culture

Ex-vivo electroporation and cortical slice culture procedures were performed on E14 embryos according to published protocol (Lizarraga et al. 2012). The culture medium used was modified from

another published protocol (De Simoni and Yu 2006). Briefly, timemated E14 embryos were harvested and immediately decapitated in ice-cold HEPES/EBSS (Gibco®). Vector constructs with 0.5 % Fast Green (Sigma) were injected into the lateral ventricle and electroporated at 42 V, 5 pulses of 50 ms at 0.1 s intervals. For knocking down Rab23, 2 μg of shControl or shRab23 were electroporated into cells. For Rab23 rescue experiment, 1.5 μg of shRab23 were co-electroporated with 2 μg WTRab23. For N-cadherin rescue experiment, 1.5 μg shRab23 was co-electroporated with 1 μg WT-N-cadherin. Electroporated cortices were isolated from the scull, embedded in 3% low-melting agarose and subjected to vibratome tissue sectioning at 250 μm thickness. Intact cortices were seeded on prewarmed cell culture inserts (Millicell®CM, PICM0RG50) and subjected to time-lapse imaging 2 days after culture.

Time-lapse Imaging and Cell Tracing Analysis

Time-lapse images were acquired using Zeiss LSM710 confocal microscopy system. EGFP-expressing cortical neurons were visualized by 488 nm laser. 48 h postculture, images were acquired at 40 min interval for 28 cycles. Images of 3–4 independent experiments were recorded. 2–3 embryos were electroporated for each group in every independent experiment. From each experiment, time-lapse videos of 5–8 cortical slices were randomly selected from each group to perform migration analysis. Migration paths of the EGFP+ neurons were manually traced and the trajectory plots were generated using ImageJ software to illustrate the migration routes of all neurons being tracked (Schneider et al. 2012). Migration distance showed was the total accumulative distance traveled by each of the neurons across the entire time frame recorded. Migration velocity showed was the average velocity of the entire migration path traveled by each of the neurons measured. Directionality was measured by comparing the Euclidean and accumulated distances, in which the value 1 represents straight-line forward migration persistency, value smaller than one reflects a migration deviation from one direction and reduce directional persistency. All analyses mentioned were performed using NIH ImageJ software with Chemotaxis Tool plugins (Schneider et al. 2012). Graphs were plotted using Graphpad Prism.

Cryosectioning, Immunohistochemistry and Imaging

Brain samples collected were fixed in 4% paraformaldehyde at 4 °C overnight, saturated in 30% sucrose in 0.12 M phosphate buffer and subjected to cryosection at 20 μm thickness. All cortices were sectioned at coronal angle and mounted on precoated glass slides (Superfrost® Plus, Fisherbrand®). Mid-coronal cortical sections were selected for immunostaining. Antibodies and the dilution factor used were: GFP (Rockland, 1:1000), Tuj1 (Covance 1:500), N-cadherin (BD Bioscience, 1:300), Tbr2 (Abcam 1:500), Ki67 (Abcam 1:500), Pax6 (Covance 1:1000), NeuN (Milipore 1:500), MAP2 (Sigma 1:800), Nestin (BD Bioscience, 1:1000), Rab23 (self-raised 1:1500) (Guo et al. 2006). Immunostaining was carried out according to standard protocols. Briefly, tissue sections were washed twice with phosphate buffer saline (PBS), permeabilized with 0.1% Tx-100, blocked 1 h in 10% horse serum and incubated 4 °C overnight with primary antibodies diluted in blocking buffer. After 3 times of 5 min washes with PBS, tissue sections were incubated with secondary antibodies (Alexa Fluor®, Life Technologies, USA) for 1 h at room temperature. Tissue sections were mounted in mounting media after 3 times PBS washes. Fluorescence images were taken using Zeiss LSM710 confocal system.

SDS-PAGE and Western Blot

Total protein lysates were extracted in ice-cold lysis buffer (40 mM Tris-HCl pH 7.5, 150 mM NaCl, 1 mM EDTA, 0.5 % Triton X-100, with freshly added protease inhibitor and PhosphoSTOP). Protein concentrations were measured by protein BCA assay (Biorad). Equal amounts of protein lysates were heat denatured and subjected to SDS-PAGE for protein size separation. After gel electrophoresis, the proteins were transferred onto blotting membrane. For immunoblotting, the blotting membrane was blocked for 1 h with 5% skimmed milk, followed by primary antibody incubation diluted in blocking buffer (5% BSA in PBS/0.1 % Tween-20) for 4 °C overnight. Membrane was washed 3 times with PBST, for 10 min each and incubated for 1 h of horseradish peroxidase (HRP) conjugated secondary antibody (Life Technologies, USA). Membrane was washed 3 times with PBST and subjected to signal development using Chemiluminescent substrate solution (Thermo Scientific Pierce). The antibodies used in this study were, anti-N-cadherin (BD Biosciences, #610 920), anti-α-tubulin (Sigma, #T5168), anti-ERK1/2 (Cell Signaling Technology, #4695), anti-pERK1/2 (Cell Signaling Technology, #4376), anti-PDGFRα (Santa Cruz, #SC-338), anti-pTyrosine (BD Transduction Laboratories, #610 000).

Real-time Quantitative

PCR. EGFP-enriched cortical tissues were isolated from E13-15 IUE brains under a fluorescence microscope. Total RNA was extracted using Qiagen's RNeasy Mini Kit. Equal amount of total RNA from each samples were subjected to reverse transcription to produce cDNA. Equal amount of cDNA was used to perform quantitative PCR assay using Biorad iQ™ SYBR® Green Supremix (#1708880). Standard QPCR protocol was carried out according to manufacturer's instruction manual. Quantification cycle, Cq values of genes of interest (i.e., *Rab23* and *N-cadherin*) were normalized to *Gapdh* reference gene (deltaCq). Relative fold change expression of KD group was obtained by normalization to the control counterpart (deltadeltaCq). Primers used were: mouse GAPDH: F-5′-TTCACCACCATGGAGAAGGC-3′, R-5′-GGCATGGACTGTGGTCATGA-3′, mouse N-cadherin: F-5′-CGGTTTCACTTGAGAGCACA-3′, R-5′-CATACGTCCCAGGCTTTGAT-3′, mouse Rab23: F-5′-AGGCCTACTATCGAGGAGCC-3′, R-5′-TTAGCCTTTTGGCCAGTCCC-3′, rat Rab23: F-5′-AGGACGTCTGTGAAGGAGGA-3′, R-5′-ACTGCTCGAATGTGTCTGCT-3′; rat N-cadherin: F-5′-GCCACCATATGACTCCCTTTTAGT-3′, R-5′-CAGAAAACTAATTCCAATCTGAAA-3′ (Chung et al. 1998); rat GAPDH: F-5′-ATGCTGGTGCTGAGTATGTC-3′, R-5′-AGTTGTCATATTTCTCGTGG-3′.

Supplementary Material

Supplementary material is available at *Cerebral Cortex* online.

Funding

This study was supported by Abbott Nutrition, the Academic Center of Excellence (ACE) research award from GlaxoSmithKline (GSK), the National Research Foundation Singapore under its Competitive Research Program grant (NRF 2008 NRF-CRP 002-082), the National Medical Research Council – Collaborative Research Grant (NMRC/CBRG/0094/2015) and Ministry of Education (MOE) Tier 2 grant (MOE2015-T2-1-022) to E.L.G.

Authors' Contributions

C.H.H. designed and performed all in vitro and in vivo experiments, analyzed data and wrote the manuscript. E.L.G. initiated

and directed the entire study, designed experiments, analyzed data and wrote the manuscript.

Notes

We thank Associate Professor B.L. Tang for constructive inputs to our study and critical reading of our manuscript, JR Ryu for the cloning of shRab23 and WTRab23 constructs, H. Liou for the cloning of shRab23 construct, W.Y. Leong for data analysis and technical support, B. Huang and J.L. Lee for data analysis and Y.S. Lim for analyzing part of the data for in vivo N-cadherin expression and helpful discussions. *Conflict of Interest*: None declared.

References

Alessandri J-L, Dagoneau N, Laville J-M, Baruteau J, Hébert J-C, Cormier-Daire V. 2010. RAB23 mutation in a large family from Comoros Islands with Carpenter syndrome. Am J Med Genet. 152A:982–986.

Azzarelli R, Kerloch T, Pacary E. 2014. Regulation of cerebral cortex development by Rho GTPases: insights from in vivo studies. Front Cell Neurosci. 8:445.

Bielas SL, Gleeson JG. 2004. Cytoskeletal-associated proteins in the migration of cortical neurons. J Neurobiol. 58:149–159.

Bystron I, Blakemore C, Rakic P. 2008. Development of the human cerebral cortex: Boulder Committee revisited. Nat Rev Neurosci. 9:110–122.

Chung SS, Mo MY, Silvestrini B, Lee WM, Cheng CY. 1998. Rat testicular N-cadherin: its complementary deoxyribonucleic acid cloning and regulation. Endocrinology. 139:1853–1862.

De Simoni A, Yu LMY. 2006. Preparation of organotypic hippocampal slice cultures: interface method. Nat Protoc. 1: 1439–1445.

Dulabon L, Olson EC, Taglienti MG, Eisenhuth S, McGrath B, Walsh CA, Kreidberg JA, Anton ES. 2000. Reelin binds alpha3beta1 integrin and inhibits neuronal migration. Neuron. 27:33–44.

Eggenschwiler JT, Espinoza E, Anderson KV. 2001. Rab23 is an essential negative regulator of the mouse Sonic hedgehog signalling pathway. Nature. 412:194–198.

Evans TM, Ferguson C, Wainwright BJ, Parton RG, Wicking C. 2003. Rab23, a negative regulator of hedgehog signaling, localizes to the plasma membrane and the endocytic pathway. Traffic. 4:869–884.

Fox JW, Lamperti ED, Ekşioğlu YZ, Hong SE, Feng Y, Graham DA, Scheffer IE, Dobyns WB, Hirsch BA, Radtke RA, et al. 1998. Mutations in filamin 1 prevent migration of cerebral cortical neurons in human periventricular heterotopia. Neuron. 21:1315–1325.

Frost EE, Zhou Z, Krasnesky K, Armstrong RC. 2009. Initiation of oligodendrocyte progenitor cell migration by a PDGF-A activated extracellular regulated kinase (ERK) signaling pathway. Neurochem Res. 34:169–181.

Geschwind DH, Rakic P. 2013. Cortical evolution: judge the brain by its cover. Neuron. 80:633–647.

Goh ELK, Young JK, Kuwako K, Tessier-Lavigne M, He Z, Griffin JW, Ming G-L. 2008. beta1-integrin mediates myelin-associated glycoprotein signaling in neuronal growth cones. Mol Brain. 1:10.

Gorski JA, Talley T, Qiu M, Puelles L, Rubenstein JL, Jones KR. 2002. Cortical excitatory neurons and glia, but not GABAergic neurons, are produced in the Emx1-expressing lineage. J Neurosci. 22:6309–6314.

Govek E-E, Hatten ME, Van Aelst L. 2011. The role of Rho GTPase proteins in CNS neuronal migration. Dev Neurobiol. 71:528–553.

Guo A, Wang T, Ng EL, Aulia S, Chong KH, Teng FYH, Wang Y, Tang BL. 2006. Open brain gene product Rab23: expression pattern in the adult mouse brain and functional characterization. J Neurosci Res. 83:1118–1127.

Hidestrand P, Vasconez H, Cottrill C. 2009. Carpenter syndrome. J Craniofac Surg. 20:254–256.

Huang T-H, Ka S-M, Hsu Y-J, Shui H-A, Tang BL, Hu K-Y, Chang J-L, Chen A. 2011. Rab23 plays a role in the pathophysiology of mesangial cells—a proteomic analysis. Proteomics. 11:380–394.

Jaglin XH, Poirier K, Saillour Y, Buhler E, Tian G, Bahi-Buisson N, Fallet-Bianco C, Phan-Dinh-Tuy F, Kong XP, Bomont P, et al. 2009. Mutations in the beta-tubulin gene TUBB2B result in asymmetrical polymicrogyria. Nat Genet. 41:746–752.

Jenkins D, Baynam G, De Catte L, Elcioglu N, Gabbett MT, Hudgins L, Hurst JA, Jehee FS, Oley C, Wilkie AOM. 2011. Carpenter syndrome: extended RAB23 mutation spectrum and analysis of nonsense-mediated mRNA decay. Hum Mutat. 32:2069–2078.

Jenkins D, Seelow D, Jehee FS, Perlyn CA, Alonso LG, Bueno DF, Donnai D, Josifova D, Josifiova D, Mathijssen IMJ, et al. 2007. RAB23 mutations in Carpenter syndrome imply an unexpected role for hedgehog signaling in cranial-suture development and obesity. Am J Hum Genet. 80:1162–1170.

Jossin Y, Cooper JA. 2011. Reelin, Rap1 and N-cadherin orient the migration of multipolar neurons in the developing neocortex. Nat Neurosci. 14:697–703.

Kawauchi T. 2011. Regulation of cell adhesion and migration in cortical neurons: not only Rho but also Rab family small GTPases. Small GTPases. 2:36–40.

Kawauchi T. 2012. Cell adhesion and its endocytic regulation in cell migration during neural development and cancer metastasis. Int J Mol Sci. 13:4564–4590.

Kawauchi T, Sekine K, Shikanai M, Chihama K, Tomita K, Kubo K-I, Nakajima K, Nabeshima Y-I, Hoshino M. 2010. Rab GTPases-dependent endocytic pathways regulate neuronal migration and maturation through N-cadherin trafficking. Neuron. 67:588–602.

Kohutek ZA, diPierro CG, Redpath GT, Hussaini IM. 2009. ADAM-10-mediated N-cadherin cleavage is protein kinase C-dependent and promotes glioblastoma cell migration. J Neurosci. 29:4605–4615.

Kriegstein AR, Noctor SC. 2004. Patterns of neuronal migration in the embryonic cortex. Trends Neurosci. 27:392–399.

Leaf A, Von Zastrow M. 2015. Dopamine receptors reveal an essential role of IFT-B, KIF17, and Rab23 in delivering specific receptors to primary cilia. Elife. 4:e06996.

Lim YS, Tang BL. 2015. A role for Rab23 in the trafficking of Kif17 to the primary cilium. J Cell Sci. 128:2996–3008.

Lizarraga SB, Coser KR, Sabbagh M, Morrow EM. 2012. Methods for study of neuronal morphogenesis: ex vivo RNAi electroporation in embryonic murine cerebral cortex. J Vis Exp. 63:e3621.

Manent J-B, Wang Y, Chang Y, Paramasivam M, LoTurco JJ. 2009. Dcx reexpression reduces subcortical band heterotopia and seizure threshold in an animal model of neuronal migration disorder. Nat Med. 15:84–90.

Martiáñez T, Lamarca A, Casals N, Gella A. 2013. N-cadherin expression is regulated by UTP in schwannoma cells. Purinergic Signal. 9:259–270.

Moon HM, Wynshaw-Boris A. 2013. Cytoskeleton in action: lissencephaly, a neuronal migration disorder. Wiley Interdiscip Rev Dev Biol. 2:229–245.

Nadarajah B, Alifragis P, Wong ROL, Parnavelas JG. 2003. Neuronal migration in the developing cerebral cortex: observations based on real-time imaging. Cereb Cortex. 13:607–611.

Nadarajah B, Brunstrom JE, Grutzendler J, Wong RO, Pearlman AL. 2001. Two modes of radial migration in early development of the cerebral cortex. Nat Neurosci. 4:143–150.

Ng T, Ryu JR, Sohn JH, Tan T, Song H, Ming G-L, Goh ELK. 2013. Class 3 semaphorin mediates dendrite growth in adult newborn neurons through Cdk5/FAK pathway. PLoS ONE. 8:e65572.

Olkkonen VM, Peterson JR, Dupree P, Lütcke A, Zerial M, Simons K. 1994. Isolation of a mouse cDNA encoding Rab23, a small novel GTPase expressed predominantly in the brain. Gene. 138:207–211.

Pellinen T, Arjonen A, Vuoriluoto K, Kallio K, Fransen JAM, Ivaska J. 2006. Small GTPase Rab21 regulates cell adhesion and controls endosomal traffic of β1-integrins. J Cell Biol. 173:767–780.

Rakic P. 1988. Specification of cerebral cortical areas. Science. 241:170–176.

Reiss K, Maretzky T, Ludwig A, Tousseyn T, de Strooper B, Hartmann D, Saftig P. 2005. ADAM10 cleavage of N-cadherin and regulation of cell–cell adhesion and β-catenin nuclear signalling. EMBO J. 24:742–752.

Schneider L, Clement CA, Teilmann SC, Pazour GJ, Hoffmann EK, Satir P, Christensen ST. 2005. PDGFRalphaalpha signaling is regulated through the primary cilium in fibroblasts. Curr Biol. 15:1861–1866.

Schneider CA, Rasband WS, Eliceiri KW. 2012. NIH Image to ImageJ: 25 years of image analysis. Nat Methods. 9:671–675.

Schrick C, Fischer A, Srivastava DP, Tronson NC, Penzes P, Radulovic J. 2007. N-cadherin regulates cytoskeletally associated IQGAP1/ERK signaling and memory formation. Neuron. 55:786–798.

Shah B, Püschel AW. 2014. In vivo functions of small GTPases in neocortical development. Biol Chem. 395:465–476.

Shih W, Yamada S. 2012. N-cadherin-mediated cell-cell adhesion promotes cell migration in a three-dimensional matrix. J Cell Sci. 125:3661–3670.

Shikanai M, Nakajima K, Kawauchi T. 2011. N-cadherin regulates radial glial fiber-dependent migration of cortical locomoting neurons. Commun Integr Biol. 4:326–330.

Spalice A, Parisi P, Nicita F, Pizzardi G, Del Balzo F, Iannetti P. 2009. Neuronal migration disorders: clinical, neuroradiologic and genetics aspects. Acta Paediatr. 98:421–433.

Stanco A, Anton ES. 2013. Radial migration of neurons in the cerebral cortex, cellular migration and formation of neuronal connections. Comprehen Dev. Neurosci. 2:317–330.

Su CTE, Yoon S-I, Marcy G, Chin EWM, Augustine GJ, Goh ELK. 2015. An optogenetic approach for assessing formation of neuronal connections in a co-culture system. J Vis Exp. 96:e52408.

Uemura K, Kihara T, Kuzuya A, Okawa K, Nishimoto T, Ninomiya H, Sugimoto H, Kinoshita A, Shimohama S. 2006. Characterization of sequential N-cadherin cleavage by ADAM10 and PS1. Neurosci Lett. 402:278–283.

Valdeolmillos M, Moya F. 2013. Leading process dynamics during neuronal migration, cellular migration and formation of neuronal connections. Comprehen Dev. Neurosci. 2:245–260.

Valiente M, Marín O. 2010. Neuronal migration mechanisms in development and disease. Curr Opin Neurobiol. 20:68–78.

Velpula KK, Rehman AA, Chelluboina B, Dasari VR, Gondi CS, Rao JS, Veeravalli KK. 2012. Glioma stem cell invasion through regulation of the interconnected ERK, integrin α6 and N-cadherin signaling pathway. Cell Signal. 24:2076–2084.

Yang X, Chrisman H, Weijer CJ. 2008. PDGF signalling controls the migration of mesoderm cells during chick gastrulation by regulating N-cadherin expression. Development. 135: 3521–3530.